ACS OMEGA

http://pubs.acs.org/journal/acsodf

Article

Beneficial Effects of lncRNA-UC.360+ shRNA on Diabetic Cardiac Sympathetic Damage via NLRP3 Inflammasome-Induced Pyroptosis in Stellate Ganglion

Liran Shi, Qixing Hu, Lin Li, Runan Yang, Xiumei Xu, Junpei Du, Lifang Zou, Guilin Li, Shuangmei Liu, Guodong Li, and Shangdong Liang*

Cite This: *ACS Omega* 2022, 7, 27714−27721

Read Online

ACCESS | Metrics & More | Article Recommendations

ABSTRACT: Hyperglycemia is one of the common symptoms of diabetes, and it produces excessive reactive oxygen species (ROS). This study investigated whether the long noncoding RNA (lncRNA) UC.360+ is involved in diabetic cardiac autonomic neuropathy (DCAN) mediated by NLRP3 inflammasome-induced pyroptosis in the stellate ganglion (SG). Using a rat type 2 diabetes model, we found that lncRNA UC.360+ short hairpin RNA (shRNA) ameliorated the dyslipidaemia of type 2 diabetic rats and reduced serum adrenaline and ROS production in SG under hyperglycemia. In addition, UC.360+ shRNA also reduced the expression of nuclear factor kappa-B (NF-κB), NLRP3, ASC, caspase-1, interleukin-1β (IL-1β), and IL-18 in the SG of diabetic rats and inhibited the phosphorylation of p38 mitogen-activated protein kinase (p38 MAPK). Therefore, lncRNA-UC.360+ shRNA may modulate the NLRP3 inflammasome/inflammatory pathway in the SG, which in turn alleviates diabetic heart sympathetic nerve damage.

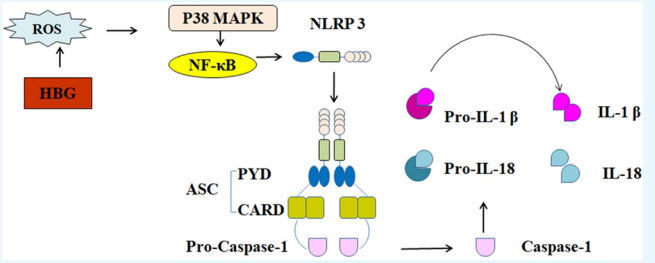

INTRODUCTION

Diabetes is characterized by hyperglycemia and is caused by the implication of both genetic and environmental risk factors. The number and prevalence of diabetes are continuously rising. Diabetic patients in China account for more than 25% of the total number of adults with diabetes in the world, which is the country with the highest number and prevalence of diabetes. In terms of the type of diabetes, the diabetes population in China is mainly the type 2, accounting for more than 90%. As the progress of disease course, it will cause complications in various tissues and organs, and diabetic cardiac autonomic neuropathy (DCAN) is one of them. DCAN in diabetic patients involves only the vagus nerve injury at the early stage, but as the disease advances, both sympathetic and parasympathetic nerves as well as myelinated and unmyelinated fibers are damaged, causing various clinical symptoms. Studies have shown that the mortality rate of DCAN patients within 5 years is more than five times of that seen in non-DCAN patients. DCAN not only reduces the living quality of diabetic patients but also has seriously negative impact on the social economy. ROS at a proper level exhibit beneficial effects by regulating intracellular signal transduction and homeostasis, while ROS at a high concentration have a damaging effect on proteins, lipids, and DNA.[1] The body's antioxidant defense system maintains the dynamic balance of ROS, and disruption of this balance either by increased ROS formation or decreased antioxidant activity in biological systems may lead to oxidative stress.[2] Increased ROS levels can promote the release of the proinflammatory transcription factor NF-κB, which mediates the occurrence of a series of diseases. ROS participate in pathological changes of diabetes implicated with cellular damage.[3] Thus, targeting oxidative stress may be a strategy to prevent and treat diabetic complications with cellular damage.

In the human transcriptome, those RNAs having no apparent protein-coding role regions are collectively referred to as noncoding RNAs (ncRNAs),[4] and the ncRNAs longer than 200 nucleotides are called long noncoding RNAs (lncRNAs). In recent years, with the progress of global transcriptome analysis, an increasing number of differential expression studies have demonstrated that lncRNAs can regulate many important biological processes, which may be implicated in the occurrence of human diseases. Among various organ systems, lncRNAs are preferentially expressed in

Received: June 9, 2022
Accepted: July 19, 2022
Published: July 29, 2022

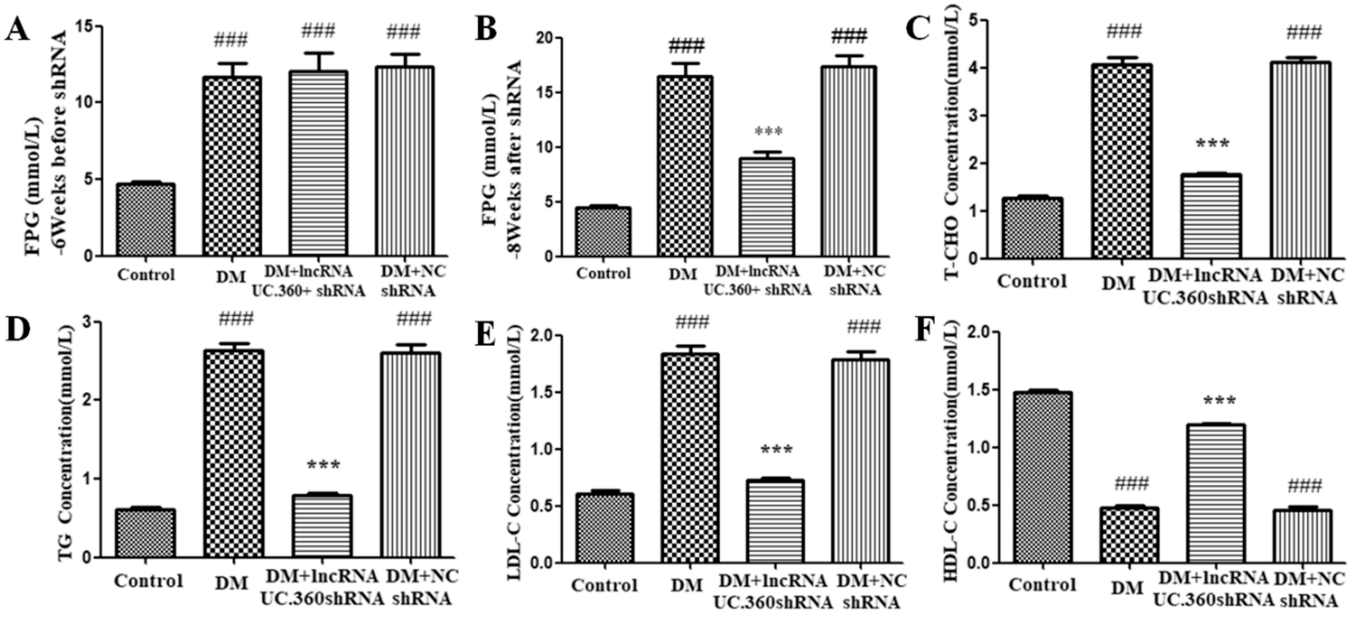

Figure 1. Effect of UC.360+ shRNA on blood glucose and lipids in DM rats. ELISA was used to detect FPG (A, B) and lipids (C−F) in each group. $^{###}p < 0.001$ vs control group, $^{***}p < 0.001$ vs DM group; $n = 3$ per group.

Table 1. Concentration of Serum Epinephrine (EPI, pg/mL) and ROS in SG Cells of Rats[a]

	control	DM	DM + uc.360+ shRNA	DM + NC shRNA
EPI content	62.13 ± 1.29	168.77 ± 7.94$^{###}$	116.17 ± 16.29***	170.20 ± 12.65$^{###}$
ROS content	62.5 ± 6.98	229.67 ± 10.65$^{###}$	82.83 ± 5.88***	231.83 ± 12.67$^{###}$

[a]$^{###}p < 0.001$ vs control, $^{***}p < 0.001$ vs DM; $n = 15$ per group.

the nervous system,[4] and consequently, the aberrant expression of lncRNAs is involved in the most devastating neurological diseases. Therefore, lncRNAs may be key players in the normal development, physiological function, and pathological changes in the nervous system. To explore the possible role of lncRNAs in nerve damage, the SOLiD Whole Transcriptome Analysis Kit was used in the early stage of this project to complete Sprague Dawley rat multi-tissue transcriptome high-throughput sequencing. Further analysis showed that many noncoding TUs in peripheral ganglion tissue have poly (A) tail structures, similar to lncRNAs. After SOLiD high-throughput sequencing, this project also identified some lncRNAs through bioinformatics predictions and molecular biology verification. A few studies showed that abnormal expression of lncRNAs is related to neurological diseases, but the mechanism of action is still unclear.[5,6] This project targeted an lncRNA (lncRNA-UC.360 as searched online) that exists in the neck sympathetic ganglia of a rat model of type 2 diabetes for experiments.

Pyroptosis can occur in vivo[7−10] and in vitro.[11] The typical features of cell pyroptosis involve these events: the plasma membrane loses its integrity, cell permeability increases, the cell membrane ruptures to form numerous small pores with a diameter of 1∼2 nm, and intracellular substances are released outside the cell.[12,13] Among the several types of inflammasomes that have been discovered, NLRP3 is linked to type 2 diabetes. The inflammasome adapter ASC self-oligomerizesto form a macromolecular complex, activates caspase-1, and then cleaves IL-1β and IL-18 precursors into active forms that can induce the synthesis of other pro-inflammatory factors and amplify local and systemic inflammatory responses.[14−16] A preliminary research showed that lncRNA-UC.360+ expression was upregulated in the stellate ganglion (SG) in type 2 diabetic rats.[17] This study established a rat model of type 2 diabetes to explore how lncRNA UC.360+ shRNA could modify hyperglycemia-induced diabetic heart sympathetic nerve damage via NLRP3 inflammasome-induced pyroptosis in SG.

RESULTS

Effect of UC.360+ shRNA on Fasting Blood Glucose (FPG) and Blood Lipids. Before UC.360+ shRNA injection (at the sixth week of the experiment), the FPG level in the diabetes mellitus (DM) group was higher than that in the control group (Figure 1A), suggesting that our model of diabetic rats was successfully established.

At the eighth week, the FPG values in the DM group was still higher than that in the control group ($p < 0.001$, Figure 1B). After UC.360+ shRNA treatment for 2 weeks, the FPG values in the DM rats was significantly reduced ($p < 0.001$, Figure 1B). The DM group did not significantly differ from the DM + NC shRNA group ($p > 0.05$, Figure 1B). Thus, UC.360+ shRNA treatment could reduce the blood glucose level of type 2 diabetic rats.

Blood lipids mainly include T-CHO, LDL-C, TG, and HDL-C. The results showed that the levels of T-CHO, TG, and LDL-C were higher in the DM group than in the control group ($p < 0.001$, Figure 1C−E). After treatment with UC.360+ shRNA, the values were significantly reduced ($p < 0.001$, Figure 1C−E). The change in the value of HDL-C was contrary to the aforementioned three lipids under the same conditions (Figure 1F). The DM group did not significantly differ from the DM + NC shRNA group ($p > 0.05$, Figure 1C−F). Our observations suggested that UC.360+ shRNA treatment could improve dyslipidaemia in type 2 diabetes.

https://doi.org/10.1021/acsomega.2c03619
ACS Omega 2022, 7, 27714−27721

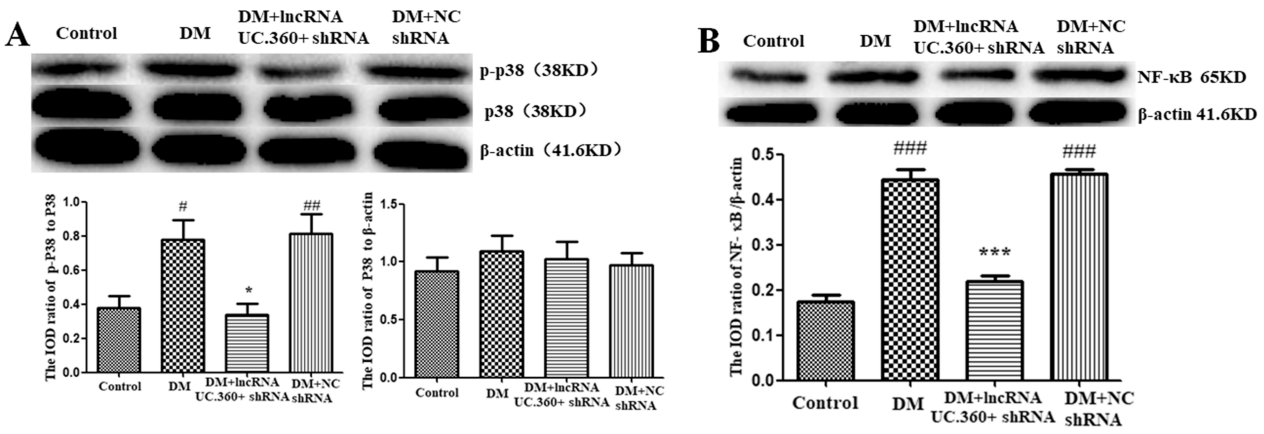

Figure 2. UC.360+ shRNA reduced the phosphorylation of p38 MAPK and content of NF-κB in the SG of DM rats. Western blotting was used to determine the protein levels of p38 MARK, p-p38 MARK (A), and NF-κB (B) in the SG. $^{\#}p < 0.05$, $^{\#\#\#}p < 0.001$ vs control group, $^{*}p < 0.05$, $^{***}p < 0.001$ vs DM group; $n = 3$ per group.

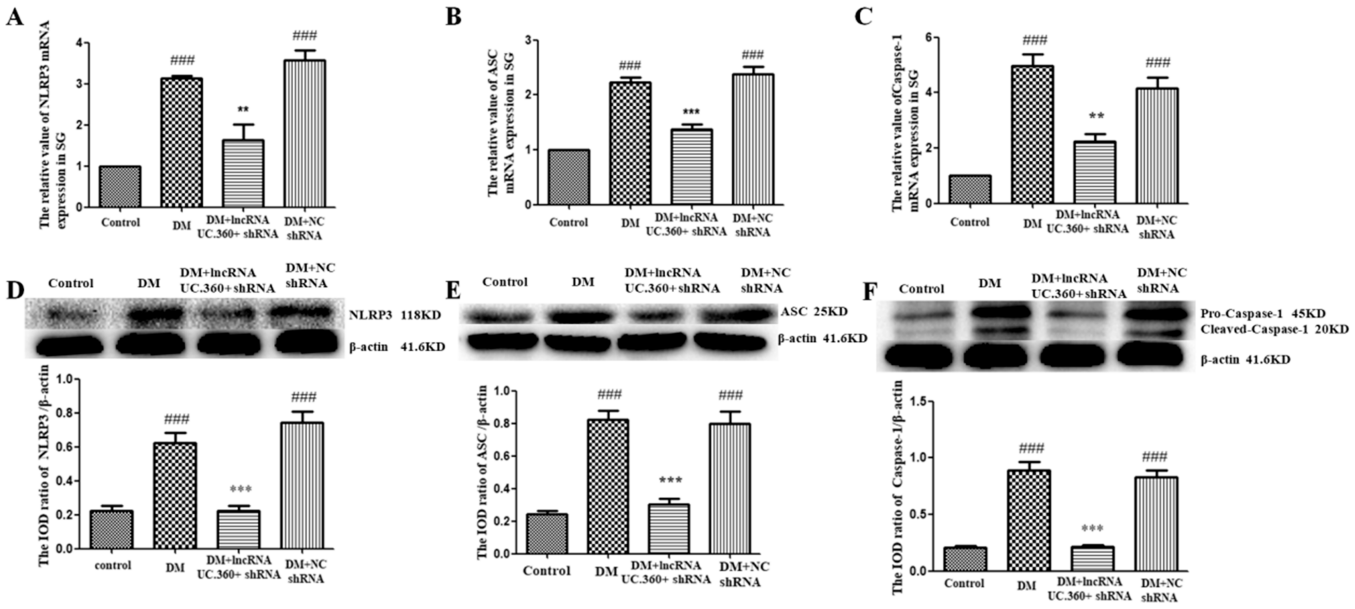

Figure 3. UC.360+ shRNA reduced the expression of NLRP3, ASC, and caspase-1 in the SG of DM rats. The expression of NLRP3, ASC, and caspase-1 mRNA (A–C) and protein (D–F) was detected by real-time quantitative PCR and Western blotting, respectively. $^{\#\#\#}p < 0.001$ vs control group, $^{**}p < 0.01$, $^{***}p < 0.001$ vs DM group; n = 3 per group.

Effect of UC.360+ shRNA on Serum Epinephrine and ROS Content. ELISA was used to detect the serum content of epinephrine (Table 1). The epinephrine content in the DM group was higher than that in the control group ($p < 0.001$). The content in the DM+ UC.360+ shRNA group was lower than that in the DM group ($p < 0.001$). The DM group did not significantly differ from the DM + NC shRNA group ($p > 0.05$).

ELISA was also used to detect the content of ROS in SG (Table 1). Our results showed that the ROS content in the DM group was higher than that in the control group ($p < 0.001$). The content was lower in the DM+ UC.360+ shRNA group than in the DM group ($p < 0.001$). The DM group did not significantly differ from the DM + NC shRNA group ($p > 0.05$). This results suggested that UC.360+ shRNA treatment inhibited ROS over-production in type 2 diabetic rats.

Effect of UC.360+ shRNA on Activation of the p38 MAPK Pathway in SG. The p38 MAPK-mediated pathway is mainly involved in stress responses. Western blotting detection found that the p38 MAPK level in the control group did not significantly differ from the DM group after normalizing by the β-actin value (Figure 2A). In contrast, the value of phospho-p38 MAPK in the DM group was higher than that in the control group ($p < 0.05$) after normalizing to the P38 value. After UC.360+ shRNA injection, the value of phospho-p38 was reduced ($p < 0.05$). The DM group did not significantly differ from the DM + NC shRNA group ($p > 0.05$).

Phosphorylation of p38 MAPK may lead to the activation of the proinflammatory transcription factor NF-κB. Western blotting detection was performed (Figure 2B), and the value of NF-κB P65 protein was normalized by β-actin. The value of NF-κB P65 protein in the DM group was higher than that in the control group ($p < 0.01$), whereas the value was lower in the DM+ UC.360+ shRNA group than in the DM group ($p < 0.001$). The DM group did not significantly differ from the DM + NC shRNA group ($p > 0.05$).

Effect of UC.360+ shRNA on Expression of NLRP3, ASC, and Caspase-1 in SG. The NLRP3 inflammatory body

https://doi.org/10.1021/acsomega.2c03619
ACS Omega 2022, 7, 27714–27721

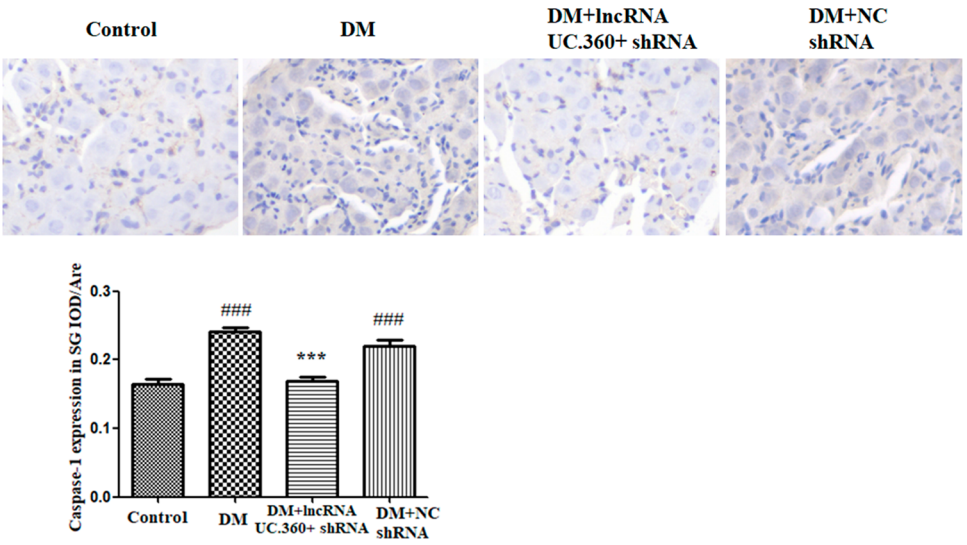

Figure 4. UC.360+ shRNA reduced the immune reactivity of caspase-1 in the SG of DM rats, as detected by immunohistochemical staining. Scale bar, 20 μm. $^{###}p < 0.001$ vs control group, $^{***}p < 0.001$ vs DM group; $n = 3$ per group.

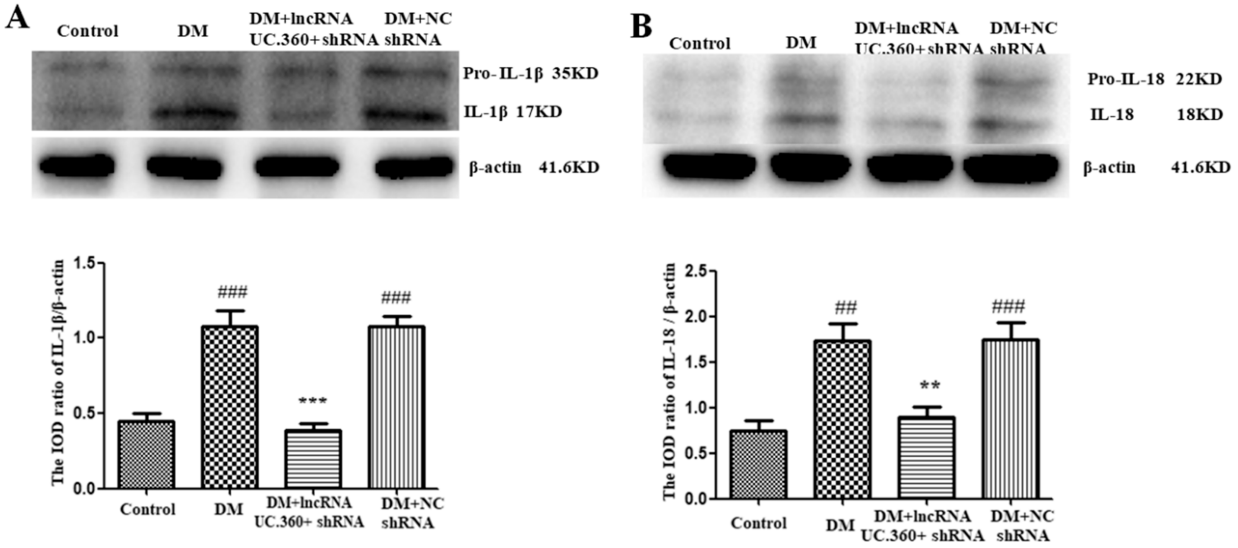

Figure 5. UC.360+ shRNA reduced the levels of IL-1β and IL-18 in the SG of DM rats. The levels of IL-1β (A) and IL-18 (B) in the SG of DM rats were detected by Western blotting. $^{##}p < 0.01$, $^{###}p < 0.001$ vs control group, $^{**}p < 0.01$, $^{***}p < 0.001$ vs DM group; $n = 3$ per group.

is a key factor inducing pyroptosis. The mRNA and protein values were standardized by β-actin. The mRNA (Figure 3A–C) and protein (Figure 3D–F) levels of NLRP3, ASC, and caspase-1 in the DM group were higher than those in the control group $p < 0.001$). The values were lower in the DM+ UC.360+ shRNA group than in the DM group ($p < 0.01$ or $p < 0.001$). The DM group did not significantly differ from the DM + NC shRNA group ($p > 0.05$).

Immunohistochemistry was performed to detect caspase-1 immune reactivity in rat SG (Figure 4). The extent of caspase-1 immune reactivity in the DM group was higher than that in the control group ($p < 0.001$). This could be significantly reduced after UC.360+ shRNA treatment ($p < 0.001$). The DM group did not significantly differ from the DM + NC shRNA group ($p > 0.05$).

Effect of UC.360+ shRNA on Expression of IL-1β and IL-18 Protein in SG. Western blotting detection showed that the levels of IL-1β and IL-18 (Figure 5A,B) in the DM group were higher than those in the control group ($p < 0.001$ for IL-1β; $p < 0.01$ for IL-18). The value was lower in the DM+ UC.360+ shRNA group than in the DM group ($p < 0.001$for IL-1β; $p < 0.01$ for IL-18). The DM group did not significantly differ from the DM + NC shRNA group ($p > 0.05$).

DISCUSSION

In this study, the detection of fasting blood glucose was used to confirm whether the rat diabetic model was successfully established. The detection of blood lipids was to validate whether lncRNA-UC.360+ shRNA could improve dyslipidemia induced by type 2 diabetes. In diabetes, the state of high glucose can prompt cells to produce excess ROS, which in turn regulates the MAPK signaling pathway and the activation of various cytokines and transcription factors. The detection of ROS in the study is not only a further confirmation of the success of the model establishment but also serves as a guiding flag in the subsequent activation of the MAPK signaling pathway. The activation of p38MAPK regulates the expression

https://doi.org/10.1021/acsomega.2c03619
ACS Omega 2022, 7, 27714−27721

of NF-κB, and NF-κB further regulates the activities of a series of components of the inflammasome NLRP3. Therefore, the experiments assessing p38 MAPK, NF-κB, NLRP3, ASC, caspase-1, IL-1β, and IL-18 by real-time PCR, Western blotting, and immunohistochemistry were followed. These experiments would reveal how lncRNA-UC.360+ shRNA treatment exhibits its potential beneficial action on counteracting the over-production of intracellular ROS and activation of the ROS-NLRP3-IL-1β signaling pathway in diabetes, thereby protecting cervical sympathetic ganglion nerve cells from pyroptosis damage.

Hyperglycemia is a typical feature of diabetes, and T2DM initially manifests as insulin resistance, which gradually progresses to β-cell damage and eventually leads to hyperglycemia. Epidemiological studies have shown that approximately 50% of type 2 diabetic patients suffer from dyslipidemia. There are studies showing that dyslipidemia also promotes the risk of developing T2DM, thus, dyslipidemia and T2DM are viewed to interact and cause each other. Therefore, in the study of type 2 diabetes, attention should be given to the phenomenon of dyslipidemia. Research has shown that LDL-C is involved in the activation of the NF-κB signaling pathway and elicits the production of ROS,[18] it can activate the NLRP3 inflammasome by upregulating pro-IL-1β in macrophages and inducing ROS production. Our results revealed that the serum contents of T-CHO, LDL-C, and TG were significantly upregulated, while HDL-C was significantly downregulated in DM rats compared with control rats. In addition, lncRNA-UC.360+ shRNA treatment effectively reversed the alterations in serum levels of these blood lipids in type 2 diabetic rats, suggesting that lncRNA-UC.360+ shRNA can improve dyslipidaemia in type 2 diabetes. In addition, upregulated epinephrine is involved in cardiac sympathetic injury.[19] LncRNA-UC.360+ shRNA counteracted the increased epinephrine due to diabetes and consequently could alleviate cardiac sympathetic injury.

ROS are relatively active oxygen-containing compounds produced by organisms in the process of aerobic metabolism, and they can also act as secondary messengers to participate in various signaling pathways, including the AKT pathway, cyclin regulation to inhibit cell proliferation, and mitochondria-mediated caspase activation/apoptosis. The unique oxidation−antioxidant system of the organism can control ROS in the body to maintain a dynamic balance under normal conditions. When the ROS in the body reach saturation, the body will lose its normal antioxidant defense ability, leading to the occurrence of various diseases. ROS can not only directly destroy cells but also stimulate signaling molecules to activate the NLRP3 inflammasome,[20] thereby mediating pyroptosis. In diabetes, the body is in a state of high glucose. High glucose can prompt cells to produce excess ROS, which in turn regulates the activation of protein kinase C, MAPK, and various cytokines and transcription factors, resulting in enhanced expression of cell-injury molecules, which ultimately leads to sympathetic neuropathy in diabetes. Therefore, reducing the content of ROS to block the ROS-activated apoptotic pathway may be a new therapeutic target for diabetic autonomic neuropathy.[21] Our data showed that the content of ROS in the SG of DM rats was significantly increased, whereas lncRNA-UC.360+ shRNA treatment could reduce the ROS overproduction in DM rats, suggesting the beneficial effect of lncRNA-UC.360+ shRNA on reducing the ROS produced at high glucose in diabetes.

The p38MAPK pathway primarily mediates the stress response and can be activated by many stimuli including ROS.[22] Activation of p38 MAPK can regulate the expression of a variety of transcription factors, including NF-κB.[23] Studies have shown that MAPK is a signal transduction factor in high glucose caused various complications of diabetes. p38 MAPK is involved in type 2 diabetic autonomic neuropathy.[24,25] This study found that the content of p38 MAPK in SG was not significantly altered, but the content of its active phosphor-p38 MAPK in SG of DM rats was upregulated, suggesting the activation of redox sensitive signal pathways. In addition, lncRNA-UC.360+ shRNA treatment decreased the content of phospho-p38 MAPK in the SG of DM rats, suggesting that lncRNA-UC.360+ shRNA could effectively inhibit the activation of the p38 MAPK signaling pathway. Moreover, the level of NF-κB protein in the SG of DM rats was increased, and it was relieved by lncRNA-UC.360+ shRNA treatment, indicating that the activation of p38 MAPK may regulate NF-κB.

Pyroptosis is accompanied by the activation of caspase-1/4/5/11,[26] and the caspase-1-induced pyroptosis is called the classical cascade.[27,28] The NLRP3 inflammasome is related to type 2 diabetes.[29] Under physiological conditions, the level of NLRP3 in the body is extremely low, NLRP3 mRNA needs to be transcribed first. At this time, NF-κB activation is required, and then translation and posttranslational modifications ensue.[30] Studies have shown that increasing the content of ROS in the cytoplasm can activate NLRP3 inflammasomes.[1,31] The high glucose in diabetes promotes the production of a large amount of ROS in the cell, which in turn can activate the NLRP3 inflammasome. NLRP3 inflammasome is a key factor in inducing pyroptosis. Cell pyroptosis is involved in diabetic nephropathy[16,32,33] and diabetic cardiomyopathy,[34,35] but the process of diabetic autonomic neuropathy induced by type 2 diabetes remains to be studied in depth. Activation of the inflammasome leads to the processing and activation of caspase-1, turning pro-caspase-1 into active caspase-1. Afterward, pro-IL-1β and pro-IL-18 are cleaved into their mature forms by caspase-1. In this study, Western blotting detected upregulated protein expression of NLRP3, ASC, caspase-1, IL-1β, and IL-18 in the SG of type 2 diabetic rats. These upregulated changes indicate inflammasome activation. LncRNA-UC.360+ shRNA treatment effectively inhibited the increase in these signaling molecules. These findings suggest that ROS may regulate the expression of NF-κB by activating the p38 MAPK signaling pathway and in turn activate the NLRP3 inflammasome to elicit pyroptosis, whereas lncRNA-UC.360+ shRNA reduced inflammasome activation and alleviated diabetic injury-mediated pyroptosis.

In conclusion, hyperglycemia in diabetes may promote the over-production of ROS in cells, and such oxidative stress can activate the p38 MAPK-mediated signaling pathway, which stimulates NF-κB and further regulates the activities of a series of components of the NLRP3 inflammasome. LncRNA-UC.360+ shRNA treatment effectively downregulated the production of intracellular ROS and inhibited the activation of the ROS-NLRP3-IL-1β signaling pathway, thereby reducing the pyroptosis of cervical sympathetic ganglion nerve cells and improving diabetic cardiac sympathetic nerve damage.

METHODS

Animals. Male Sprague−Dawley rats weighing 180−220 g were purchased from Changsha Tianqin Experimental Animal

https://doi.org/10.1021/acsomega.2c03619
ACS Omega 2022, 7, 27714−27721

Center. The animal operation protocol was reviewed and approved by the Ethics Committee of Medical School of Nanchang University. The rats were placed in clean cages, and the room was kept at 22 ± 2 °C and 50% humidity. After adaptation, the rats were randomly divided into a control group and a DM group. After 4 weeks of feeding with a high-sugar and high-fat diet, rats for type 2 diabetic model were injected intraperitoneally (i.p.) with streptozotocin (STZ) (30 mg/kg). The establishment of a rat diabetic model and drug treatment were performed as previously described.[17] In short, in this experiment, rats were fed a high-sugar and high-fat diet to induce insulin resistance. Later, a small dose of STZ was injected i.p. to impair the islet function and reduce insulin secretion. Without sufficient insulin levels, the body cannot maintain normal blood sugar levels, thus establishing a rat model of type 2 diabetes.

Blood Glucose. A Roche blood glucose meter was used to measure blood glucose after 12 h of fasting (fasting at 21:00 the night before, blood glucose measurement at 9:00 the next morning, free drinking). After the tail of the rat was sterilized and approximately 3 mm of tail tip was cut off, the blood was dropped onto the blood glucose test paper that was inserted into the meter to read the value of blood glucose. After waiting for 2 s, the blood glucose value was read on the blood glucose meter and recorded.

Blood Lipids. Fresh blood was collected and kept at 25 °C for 30 min. The samples were centrifuged at 2000 × *g* for 15 min at 4 °C, and the upper layer of pale-yellow clear liquid was serum. The serum was collected in disposable endotoxin-free test tubes and kept on ice for testing. If serum could not be tested on the same day, it was stored at −80 °C until use. The contents of T-CHO, TG, LDL-C, and HDL-C in the serum of rats were measured by assay kits (Elabscience Biotechnology, China).

Epinephrine (EPI). Blood collection was conducted as described above. The serum adrenaline concentration of rats was measured according to the kit instructions (Elabscience Biotechnology, China). This kit uses a competitive ELISA method. The EPI antigen is coated on the ELISA plate. During the measurement, the EPI in the sample or standard competes with the coated EPI to bind to the site on the biotin-labeled anti-EPI monoclonal antibody. Horseradish peroxidase-labeled avidin was added, and after the reaction, the EPI concentration was measured.

ROS. Fresh SG tissue was placed in precooled PBS to remove other impurities around the tissue. After cutting the SG into 1 mm^3 pieces, a certain amount of pancreatin was added for digestion (37 °C, 30 min). The digestion was stopped with precooled PBS, and the samples were passed through a 300-mesh nylon mesh to remove tissue blocks and then centrifuged (1500 × *g*, 10 min). The supernatant was removed, and a single-cell suspension was obtained. The total number of cells used for fluorescence detection was ensured to be greater than 10^6. The wavelength settings were as follows: excitation light of 500 nm and emission wavelength of 525 nm, the value obtained was the fluorescence value needed.

Real-Time PCR. After the diabetic model was established, the SG tissue was separated and washed in PBS to remove residual blood. The extraction kit was used for RNA extraction (Beijing TransGen Biotech Co. Beijing, China). After the sample was lysed by TRIzol and layered with chloroform, isopropanol and absolute ethanol were added successively for precipitation to obtain high-purity total RNA. Then, the instructions of the cDNA synthesis kit were followed to reverse transcribe the required cDNA (Thermo Fisher Scientific, USA). The total of 20 μL cDNA reverse transcription reaction system was set up according to the steps as follows: 4 μL of 5 × buffer, 2 μL of dNTPs, 1 μL of OligDT, 1 μL of MMLV, 1 μL of RNasin, and 11 μL of RNA sample, they were mixed well in a 37 °C water bath for 1 h.

PCR system was configured according to the Promage instructions. Each primer and each cDNA template were added to three replicate wells, and each well was 20 μL, which included the following reaction components: 7 μL of ribozyme-free water, 0.5 μL of both upstream and downstream primers, 10 μL of 2 × Master Mix, and 2 μL of cDNA. The primer sequences are shown in Table 2.

Table 2. Primer Sequences

β-actin	forward:	5′- TAAAGACCTCTATGCCAACACAGT −3′
	reverse:	5′- CACGATGGAGGGGCCGGACTCATC -3′
NLRP3	forward:	5′-CTGCATGCCGTATCTGGTTG −3′
	reverse:	5′-CGGCGTTAGCAGAAATCCAG-3′
ASC	forward:	5′-CTCTGTATGGCAATGTGCTGAC-3′
	reverse:	5′-GAACAAGTTCTTGCAGGTCAG-3′
caspase-1	forward:	5′-GGAGCTTCAGTCAGGTCCAT −3′
	reverse:	5′-GCGCCACCTTCTTTGTTCAG −3′

Western Blotting. The previously separated SG tissue was removed from −80 °C and ground with a homogenizer after 300 μL of lysate was added (the homogenizer was soaked in acid overnight, autoclaved, and used after drying, the whole procedure was performed on ice). The milled homogenate was transferred to a precooled EP tube and centrifuged. The supernatant was collected. Loading buffer was added according to the proportion, mixed and sealed, and boiled in boiling water until denatured. After cooling, the samples were transferred to −20 °C for storage. SDS−PAGE of the corresponding specifications was performed as required. After BCA quantification of protein content, 15 μL of the protein sample was added to each well. Gel electrophoresis was performed at 20 mA/gel for approximately 2 h. Then, the membrane was transferred to a constant current of 300 mA in an ice bath, and the transfer time was approximately 90 min. The blots on the membrane were incubated with primary and secondary antibodies and placed in a gel imager for development. The following primary antibodies (dilution ratio of 1:1000) were used: rabbit anti-p-p38 MAPK and rabbit anti-p38 MAPK (Cell Signaling Technology, Beverly, MA), rabbit anti-NF-*κ*BP65 and rabbit anti-ASC (Affinity, Cincinnati, OH, USA), rabbit anti-Pro-Caspase-1 (Novus Biologicals, USA), rabbit anti-NLRP3, rabbit anti-Pro-IL-1*β* and rabbit anti-Pro-IL-18 (Abcam, UK), and mouse anti-*β*-actin (ZSGB-Bio, Beijing, China). Anti-mouse IgG and goat anti-rabbit IgG (ZSGB-Bio, Beijing, China) were used as the secondary antibodies with a dilution ratio of 1:2000. The optical density (OD) values were analyzed by ImageJ.

Immunohistochemistry. The isolated rat SG was fixed in 4% PFA, and then 10 μm frozen slices were prepared. The slices were deparaffinized and rehydrated after incubation with 3% H_2O_2 (10 min). The slices were blocked with 3% BSA for 90 min and incubated with rabbit anti-caspase 1 antibody (1200) overnight. Afterward, the slices were incubated with a secondary antibody for 2 h. The slides were mounted with neutral gum, and images were captured under a microscope.

https://doi.org/10.1021/acsomega.2c03619
ACS Omega 2022, 7, 27714−27721

Statistical Analysis. SPSS 21 and Origin 9.0 were used for data analysis. Prism 5.0 was used for data graphing. One-way ANOVA was used for comparisons between two or more data points, and the LSD method was used for comparisons between groups. Values are presented as the mean ± SD. $P < 0.05$ was defined as significant.

AUTHOR INFORMATION

Corresponding Author

Shangdong Liang − *Neuropharmacology Laboratory of Physiology Department, Basic Medical School of Nanchang University, Nanchang 330006, PR China; Jiangxi Provincial Key Laboratory of Autonomic Nervous Function and Disease, Nanchang, Jiangxi 330006, PR China;* orcid.org/0000-0003-0903-3004; Email: liangsd@hotmail.com

Authors

Liran Shi − *Neuropharmacology Laboratory of Physiology Department, Basic Medical School of Nanchang University, Nanchang 330006, PR China; The people's hospital of Jiawang of Xuzhou, Xuzhou 221011, China; Jiangxi Provincial Key Laboratory of Autonomic Nervous Function and Disease, Nanchang, Jiangxi 330006, PR China*

Qixing Hu − *Neuropharmacology Laboratory of Physiology Department, Basic Medical School of Nanchang University, Nanchang 330006, PR China; Jiangxi Provincial Key Laboratory of Autonomic Nervous Function and Disease, Nanchang, Jiangxi 330006, PR China*

Lin Li − *Neuropharmacology Laboratory of Physiology Department, Basic Medical School of Nanchang University, Nanchang 330006, PR China; Jiangxi Provincial Key Laboratory of Autonomic Nervous Function and Disease, Nanchang, Jiangxi 330006, PR China*

Runan Yang − *Neuropharmacology Laboratory of Physiology Department, Basic Medical School of Nanchang University, Nanchang 330006, PR China; Jiangxi Provincial Key Laboratory of Autonomic Nervous Function and Disease, Nanchang, Jiangxi 330006, PR China*

Xiumei Xu − *Neuropharmacology Laboratory of Physiology Department, Basic Medical School of Nanchang University, Nanchang 330006, PR China; Jiangxi Provincial Key Laboratory of Autonomic Nervous Function and Disease, Nanchang, Jiangxi 330006, PR China*

Junpei Du − *Neuropharmacology Laboratory of Physiology Department, Basic Medical School of Nanchang University, Nanchang 330006, PR China; Jiangxi Provincial Key Laboratory of Autonomic Nervous Function and Disease, Nanchang, Jiangxi 330006, PR China*

Lifang Zou − *Neuropharmacology Laboratory of Physiology Department, Basic Medical School of Nanchang University, Nanchang 330006, PR China; Department of Haematology, The First Affiliated Hospital of Nanchang University, Nanchang, Jiangxi 330006, China; Jiangxi Provincial Key Laboratory of Autonomic Nervous Function and Disease, Nanchang, Jiangxi 330006, PR China*

Guilin Li − *Neuropharmacology Laboratory of Physiology Department, Basic Medical School of Nanchang University, Nanchang 330006, PR China; Jiangxi Provincial Key Laboratory of Autonomic Nervous Function and Disease, Nanchang, Jiangxi 330006, PR China*

Shuangmei Liu − *Neuropharmacology Laboratory of Physiology Department, Basic Medical School of Nanchang University, Nanchang 330006, PR China; Jiangxi Provincial Key Laboratory of Autonomic Nervous Function and Disease, Nanchang, Jiangxi 330006, PR China*

Guodong Li − *Neuropharmacology Laboratory of Physiology Department, Basic Medical School of Nanchang University, Nanchang 330006, PR China; Jiangxi Provincial Key Laboratory of Autonomic Nervous Function and Disease, Nanchang, Jiangxi 330006, PR China*

Complete contact information is available at: https://pubs.acs.org/10.1021/acsomega.2c03619

Author Contributions

All authors approved the final version of manuscript. S.D.L., L.R.S., and G.D.L. conceived and designed the research, and drafted the manuscript. L.R.S. performed the statistical analysis and interpreted the data. L.R.S., Q.X.H., L.L., R.N.Y., X.M.X. J.P.D., L.F.Z. G.L.L. and S.M.L. performed the experiments.

Funding

This work was supported by grants from the National Natural Science Foundation of China (81870574, 81970749, 8181101216, 82160163, 82160253, 81570735, 31560276, 81560219, 81860217, and 81701114), the Science and Technology Key Program Founded by the Education Department of Jiangxi Province (GJJ190015), the Key Research and Development programs of Jiangxi Province (20192BBH80017), the Scientific Research Cultivation Project for Young Teachers founded by Medical college of Nanchang University (PY201920) and the Youth Medical Science and Technology Innovation Project of Xuzhou City (XWKYHT20200009).

Notes

The authors declare no competing financial interest.

ABBREVIATIONS

ROS reactive oxygen species; LncRNA long noncoding RNA; DCAN diabetic cardiac autonomic neuropathy; SG stellate ganglion; NLRP3 NOD-like receptor thermal protein domain associated protein 3; ASC apoptosis-associated Speck-like protein containing a CARD; NF-κB nuclear factor kappa-B; IL-1β interleukin-1β; IL-18 interleukin-18; p38 MAPK p38 mitogen-activated protein kinase; DM diabetes mellitus; ELISA enzyme-linked immunosorbent assay

REFERENCES

(1) Abais, J. M.; Xia, M.; Zhang, Y.; Boini, K. M.; Li, P. L. Redox regulation of NLRP3 inflammasomes: ROS as trigger or effector? *Antioxid. Redox Signaling* **2015**, *22*, 1111−1129.

(2) Li, R.; Jia, Z.; Trush, M. A. Defining ROS in Biology and Medicine. *React. Oxygen Species* **2016**, *1*, 9−21.

(3) Byrne, N. J.; Rajasekaran, N. S.; Abel, E. D.; Bugger, H. Therapeutic potential of targeting oxidative stress in diabetic cardiomyopathy. *Free Radical Biol. Med.* **2021**, *169*, 317−342.

(4) Militello, G.; Weirick, T.; John, D.; Doring, C.; Dimmeler, S.; Uchida, S. Screening and validation of lncRNAs and circRNAs as miRNA sponges. *Brief Bioinform.* **2017**, *18*, 780−788.

(5) Ramos, A. D.; Attenello, F. J.; Lim, D. A. Uncovering the roles of long noncoding RNAs in neural development and glioma progression. *Neurosci. Lett.* **2016**, *625*, 70−79.

(6) Khorkova, O.; Hsiao, J.; Wahlestedt, C. Basic biology and therapeutic implications of lncRNA. *Adv. Drug Delivery Rev.* **2015**, *87*, 15−24.

(7) Gao, L.; Dong, X.; Gong, W.; Huang, W.; Xue, J.; Zhu, Q.; Ma, N.; Chen, W.; Fu, X.; Gao, X.; Lin, Z.; Ding, Y.; Shi, J.; Tong, Z.; Liu, T.; Mukherjee, R.; Sutton, R.; Lu, G.; Li, W. Acinar cell NLRP3 inflammasome and gasdermin D (GSDMD) activation mediates

pyroptosis and systemic inflammation in acute pancreatitis. *Br. J. Pharmacol.* **2021**, *178*, 3533−3552.
(8) Shu, B.; Zhou, Y. X.; Li, H.; Zhang, R. Z.; He, C.; Yang, X. The METTL3/MALAT1/PTBP1/USP8/TAK1 axis promotes pyroptosis and M1 polarization of macrophages and contributes to liver fibrosis. *Cell death discovery.* **2021**, *7*, 368.
(9) Xu, P.; Hong, Y.; Xie, Y.; Yuan, K.; Li, J.; Sun, R.; Zhang, X.; Shi, X.; Li, R.; Wu, J.; Liu, X.; Hu, W.; Sun, W. TREM-1 Exacerbates Neuroinflammatory Injury via NLRP3 Inflammasome-Mediated Pyroptosis in Experimental Subarachnoid Hemorrhage. *Transl. Stroke Res.* **2021**, *12*, 643−659.
(10) Yuan, R.; Zhao, W.; Wang, Q. Q.; He, J.; Han, S.; Gao, H.; Feng, Y.; Yang, S. Cucurbitacin B inhibits non-small cell lung cancer in vivo and in vitro by triggering TLR4/NLRP3/GSDMD-dependent pyroptosis. *Pharmacol. Res.* **2021**, *170*, No. 105748.
(11) Zeng, W.; Wu, D.; Sun, Y.; Suo, Y.; Yu, Q.; Zeng, M.; Gao, Q.; Yu, B.; Jiang, X.; Wang, Y. The selective NLRP3 inhibitor MCC950 hinders atherosclerosis development by attenuating inflammation and pyroptosis in macrophages. *Sci. Rep.* **2021**, *11*, 19305.
(12) Byrne, B. G.; Dubuisson, J. F.; Joshi, A. D.; Persson, J. J.; Swanson, M. S. Inflammasome components coordinate autophagy and pyroptosis as macrophage responses to infection. *MBio* **2013**, *4*, e00620−e00612.
(13) Gage, J.; Hasu, M.; Thabet, M.; Whitman, S. C. Caspase-1 deficiency decreases atherosclerosis in apolipoprotein E-null mice. *Can J Cardiol.* **2012**, *28*, 222−229.
(14) Hong, L.; Zha, Y.; Wang, C.; Qiao, S.; An, J. Folic Acid Alleviates High Glucose and Fat-Induced Pyroptosis via Inhibition of the Hippo Signal Pathway on H9C2 Cells. *Front. Mol. Biosci.* **2021**, *8*, No. 698698.
(15) Jiao, Y.; Nan, J.; Mu, B.; Zhang, Y.; Zhou, N.; Yang, S.; Zhang, S.; Lin, W.; Wang, F.; Xia, A.; Cao, Z.; Chen, P.; Pan, Z.; Lin, G.; Pan, S.; Bin, H.; Li, L.; Yang, S. Discovery of a novel and potent inhibitor with differential species-specific effects against NLRP3 and AIM2 inflammasome-dependent pyroptosis. *Eur. J. Med. Chem.* **2022**, *232*, No. 114194.
(16) Wang, W.; Cao, Z.; Liang, H.; Zhao, C.; Gong, B.; Hu, J. Effect of low-dose ethanol on NLRP3 inflammasome in diabetes-induced lung injury. *Exp. Anim.* **2021**, *70*, 364−371.
(17) Shi, L.; Sun, M.; Ren, X.; Li, Z.; Yang, R.; Xu, X.; Li, L.; Li, G.; Liu, S.; Schmalzing, G.; Nie, H.; Li, G.; Liang, S. LncRNA UC.360+ shRNA Improves Diabetic Cardiac Sympathetic Dysfunction Mediated by the P2X4 Receptor in the Stellate Ganglion. *ACS Chem. Neurosci.* **2021**, *12*, 1210−1218.
(18) Yurdagul, A., Jr.; Sulzmaier, F. J.; Chen, X. L.; Pattillo, C. B.; Schlaepfer, D. D.; Orr, A. W. Oxidized LDL induces FAK-dependent RSK signaling to drive NF-kappaB activation and VCAM-1 expression. *J. Cell Sci.* **2016**, *129*, 1580−1591.
(19) Zhang, J.; Liu, S.; Xu, B.; Li, G.; Li, G.; Huang, A.; Wu, B.; Peng, L.; Song, M.; Xie, Q.; Lin, W.; Xie, W.; Wen, S.; Zhang, Z.; Xu, X.; Liang, S. Study of baicalin on sympathoexcitation induced by myocardial ischemia via P2X3 receptor in superior cervical ganglia. *Auton Neurosci.* **2015**, *189*, 8−15.
(20) Song, W.; Wei, L.; Du, Y.; Wang, Y.; Jiang, S. Protective effect of ginsenoside metabolite compound K against diabetic nephropathy by inhibiting NLRP3 inflammasome activation and NF-κB/p38 signaling pathway in high-fat diet/streptozotocin-induced diabetic mice. *Int. Immunopharmacol.* **2018**, *63*, 227−238.
(21) Yang, X.; Li, X.; Zhu, Y.; Gao, Y.; Xu, L. Paeoniflorin Upregulates Mitochondrial Thioredoxin of Schwann Cells to Improve Diabetic Peripheral Neuropathy Indicated by 4D Label-Free Quantitative Proteomics. *Oxid. Med. Cell. Longevity* **2022**, *2022*, 4775645.
(22) Sato, A.; Okada, M.; Shibuya, K.; Watanabe, E.; Seino, S.; Narita, Y.; Shibui, S.; Kayama, T.; Kitanaka, C. Pivotal role for ROS activation of p38 MAPK in the control of differentiation and tumor-initiating capacity of glioma-initiating cells. *Stem Cell Res.* **2014**, *12*, 119−131.
(23) Li, J. S.; Ji, T.; Su, S. L.; Zhu, Y.; Chen, X. L.; Shang, E. X.; Guo, S.; Qian, D. W.; Duan, J. A. Mulberry leaves ameliorate diabetes via regulating metabolic profiling and AGEs/RAGE and p38 MAPK/NF-κB pathway. *J. Ethnopharmacol.* **2022**, *283*, No. 114713.
(24) Guo, J.; Sheng, X.; Dan, Y.; Xu, Y.; Zhang, Y.; Ji, H.; Wang, J.; Xu, Z.; Che, H.; Li, G.; Liang, S.; Li, G. Correction to: Involvement of P2Y12 receptor of stellate ganglion in diabetic cardiovascular autonomic neuropathy. *Purinergic Signal.* **2021**, *17*, 163.
(25) Sheng, X.; Wang, J.; Guo, J.; Xu, Y.; Jiang, H.; Zheng, C.; Xu, Z.; Zhang, Y.; Che, H.; Liang, S.; Zhu, G.; Li, G. Effects of Baicalin on Diabetic Cardiac Autonomic Neuropathy Mediated by the P2Y12 Receptor in Rat Stellate Ganglia. *Cell. Physiol. Biochem.* **2018**, *46*, 986−998.
(26) Wang, S.; Pacher, P.; De Lisle, R. C.; Huang, H.; Ding, W. X. A Mechanistic Review of Cell Death in Alcohol-Induced Liver Injury. *Alcohol Clin Exp Res.* **2016**, *40*, 1215−1223.
(27) Sun, Q.; Scott, M. J. Caspase-1 as a multifunctional inflammatory mediator: noncytokine maturation roles. *J. Leukocyte Biol.* **2016**, *100*, 961−967.
(28) Yogarajah, T.; Ong, K. C.; Perera, D.; Wong, K. T. AIM2 Inflammasome-Mediated Pyroptosis in Enterovirus A71-Infected Neuronal Cells Restricts Viral Replication. *Sci. Rep.* **2017**, *7*, 5845.
(29) Baldwin, A. G.; Brough, D.; Freeman, S. Inhibiting the Inflammasome: A Chemical Perspective. *J. Med. Chem.* **2016**, *59*, 1691−1710.
(30) Li, Y.; Xie, H.; Zhang, H. Protective effect of sinomenine against inflammation and oxidative stress in gestational diabetes mellitus in female rats via TLR4/MyD88/NF-kappaB signaling pathway. *J. Food Biochem.* **2021**, *45*, No. e13952.
(31) Aminzadeh, M.; Roghani, M.; Sarfallah, A.; Riazi, G. H. TRPM2 dependence of ROS-induced NLRP3 activation in Alzheimer's disease. *Int. Immunopharmacol.* **2018**, *54*, 78−85.
(32) Guo, H.; Bi, X.; Zhou, P.; Zhu, S.; Ding, W. NLRP3 Deficiency Attenuates Renal Fibrosis and Ameliorates Mitochondrial Dysfunction in a Mouse Unilateral Ureteral Obstruction Model of Chronic Kidney Disease. *Mediators Inflamm.* **2017**, *2017*, 8316560.
(33) Zhang, L.; Jing, M.; Liu, Q. Crocin alleviates the inflammation and oxidative stress responses associated with diabetic nephropathy in rats via NLRP3 inflammasomes. *Life Sci.* **2021**, *278*, No. 119542.
(34) Song, S.; Ding, Y.; Dai, G. L.; Zhang, Y.; Xu, M. T.; Shen, J. R.; Chen, T. T.; Chen, Y.; Meng, G. L. Sirtuin 3 deficiency exacerbates diabetic cardiomyopathy via necroptosis enhancement and NLRP3 activation. *Acta Pharmacol. Sin.* **2021**, *42*, 230−241.
(35) Sun, Y.; Ding, S. NLRP3 Inflammasome in Diabetic Cardiomyopathy and Exercise Intervention. *Int. J. Mol. Sci.* **2021**, *22*, 13228.

https://doi.org/10.1021/acsomega.2c03619
ACS Omega 2022, 7, 27714−27721